1   **Chrysomycin A inhibits the topoisomerase I of *Mycobacterium tuberculosis*.**

2   Balaji Muralikrishnan[1], Lekshmi K. Edison[1], Azger Dusthackeer[2], Jijimole G R[1], Ranjit

3   Ramachandran[1], Aravind Madhavan[1], Ajay Kumar Ramakrishnan[1*].

4   [1]Mycobacterium Research Laboratory, Rajiv Gandhi Centre for Biotechnology,
5   Thiruvananthapuram, Kerala, India.

6   [2]Department of Bacteriology, National Institute for Research in Tuberculosis, Chennai, Tamil
7   Nadu, India.

8   [*]Corresponding author. Email id: rakumar@rgcb.res.in

9   **Abstract**

10   Novel anti-tuberculosis drugs are essential to manage drug resistant tuberculosis, caused by the

11   notorious pathogen *Mycobacterium tuberculosis.* We recently reported the antimycobacterial

12   activity of chrysomycin A in vitro and in infected macrophages. In this study, we report that the

13   molecule inhibits the growth of drug resistant clinical strains of *Mycobacterium tuberculosis* and

14   acts in synergy with anti-TB drugs such as ethambutol, ciprofloxacin and novobiocin. In pursuit

15   of its mechanism of action, it was found that chrysomycin A renders bactericidal activity by

16   interacting with DNA at specific sequences and by inhibiting topoisomerase I activity of

17   *Mycobacterium tuberculosis*. It also exhibits weak inhibition of gyrase enzyme of the pathogen.

18   **Introduction**

19   Chrysomycin A was first discovered by Strelitz et al., in 1955 when screening extracts of

20   actinomycetes against bacteriophages [1]. Although it was discovered in the golden era of

21   antibiotic discovery, it remained non-available. A few studies have reported its anti-

22   tumorigenicnature [2-4]. Acetylated forms of chrysomycins were also reported for the same activity

23   [5]. However, our laboratory was the first one to report chrysomycin A's anti-*Mycobacterium*

24   *tuberculosis* property. In our drug screening program against *M. tuberculosis*, we chanced upon

25   chrysomycin A from a novel *Streptomyces* sp [6]. It has bactericidal activity on both planktonic as

26   well as phagocytosed bacteria. Subsequently in an independent study, derivatives of

27   chrysomycin A have been reported for strong growth inhibitory activity against drug resistant *M.*

28   *tuberculosis* [7]. Structurally, chrysomycin A is a napthocoumarin and has a planar structure and

1

29   this led us to speculate about its interaction with DNA [8, 9]. Identification of the target of

30   chrysomycin A in *M. tuberculosis* is essential to understand its mechanism of action which

31   ultimately could lead to rational design of potent molecules from its chemical backbone.

32   This study focuses on identifying the target of chrysomycin A in *M. tuberculosis*. Towards this,

33   we tested the molecule on various drug resistant clinical strains of *M. tuberculosis* to draw initial

34   cues from the drug resistance pattern. Subsequently, DNA interaction studies were carried out

35   using physico-chemical methods and molecular docking analysis. The results were suggestive of

36   inhibition of topoisomerases and to check this possibility, functional inhibition assays were

37   performed and support was drawn from molecular docking analysis.

Materials and Methods

Bacterial strains, cell lines, chemicals and general procedures

40   *M. tuberculosis* H37Rv was grown on Middlebrook 7H9 medium (BD Difco, New Jersey)

41   supplemented with 10% Oleic acid-Albumin-Dextrose-Catalase (OADC, Difco). The details of

42   the drug resistant clinical strains of *M. tuberculosis* are provided in the Table 1. Middlebrook

43   7H10 solid medium was procured from BD Difco, while flat opti bottom 96 well plates were

44   from ThermoFisher Scientific, Massachusetts, United States. *M. tuberculosis* gyrase and

45   topoisomerase I inhibition kits were bought from Inspiralis (Norwich, UK). Potssium iodide,

46   Sodium chloride and oligonucleotides (listed in supplementary table 2) were procured from

47   Sigma (India)

Antimicrobial activity of chrysomycin A on drug resistant clinical strains of *M. tuberculosis*

49   Chrysomycin A was tested on drug resistant clinical strains of *M. tuberculosis*. For this, well

50   characterized mono-drug resistant, multidrug resistant and extensively drug resistant strains were

51   used and micro-dilution assay was performed on each (1-16 µg/mL). After incubating the culture

52   at 37 °C for 24 h, 5 µL of the treated and control cultures were spotted onto Middlebrook 7H10

53   solid medium. The lowest concentration at which no colonies appeared was considered as the

54   MIC.

Study of synergism with anti-TB drugs

56 To check whether chrysomycin A can interact with some of the current anti-TB drugs, checker
57 board assay was performed as described [10]. Surrogate organism, *Mycobacterium smegmatis,* was
58 used for this particular experiment. First-line drugs, isoniazid, rifampicin and ethambutol were
59 included in the study along with ciprofloxacin and novobiocin. Pyrazinamide, a first-line drug
60 was not included in the study as the drug is not active against *M. smegmatis*. In the checker board
61 assay, synergy between chrysomycin A and the first-line drugs in eliciting antimicrobial property
62 was determined individually. Briefly, as shown in Figure S2A, in a 96 well plate, chrysomycin
63 A was serially diluted (6 µg/mL to 1/16 µg/mL) in horizontal direction from left to right until the
64 penultimate column and leaving the wells in the last column without chrysomycin A. Next, the
65 second line drug (ciprofloxacin, as shown in Figure 32A) is serially diluted (1 µg/mL to 1/16
66 µg/mL) in the vertical direction from top to bottom until the penultimate row leaving the last row
67 without ciprofloxacin. Thus, the last row and the last column will indicate the individual MIC of
68 chrysomycin A and ciprofloxacin, respectively. The test organism, *M. smegmatis* $(1.5 \times 10^6$
69 bacteria) was inoculated and resazurin microtitre assay was performed as described [11]. The wells
70 between the last row and last column of the 96 well plate bear the different combinations of both
71 the drugs.

Fluorescence spectrometry

73 The experiment was performed as described by Rehman et al [12] with minor changes. Briefly, flat
74 opti-bottom Nunc 96 well plates were used instead of cuvettes. Chrysomycin A (5 or 50 µM)
75 was kept at constant concentration and its intrinsic fluorescence was read between 400 and 600
76 nm when excited at 280 nm. Increasing concentrations (0-50µM) of calf thymus DNA or short
77 stretches of single/double stranded DNA were added to this, and the change in fluorescence
78 spectrum was monitored. The spectra were read using JASCON fluorometer and the graph was
79 plotted using Graphpad Prism version 7 Software. Stern-Volmer quenching constant was
80 calculated from the slope of $[F/F_0]$ vs [DNA] plot. F_0 is the initial fluorescence before adding
81 potassium iodide and F is the fluorescence obtained after addition, while [DNA] is the
82 concentration of DNA. The constant was compared to that of reported intercalators and groove
83 binders [13].

Effect of potassium iodide and sodium chloride on the fluorescence of DNA-chrysomycinA complex

3

86   Potassium iodide quenching was carried out as described by Sadeghi et al [14]. Briefly, potassium
87   iodide (0–8 mM) was added to chrysomycin A (50 μM) and DNA-chrysomycin complex (10 μM
88   of double stranded DNA with 50 μM of chrysomycin A). The total reaction volume was 200 μL.
89   After exciting at 280 nm, the fluorescence emission spectra were recorded between 400 to 600
90   nm. A graph was plotted with the ratios of F and F_0 against increasing concentrations of
91   potassium iodide. The effect of ionic strength was studied by varying the concentration of
92   sodium chloride between 0 and 70 mM in a total volume of 200 μL containing 50 μM
93   chrysomycin A or calf thymus DNA-chrysomycin A complex (1:1). The change in spectrum was
94   recorded at 505 nm and a graph was plotted against increasing concentrations of sodium
95   chloride.

Circular dichroism (CD)

97   CD spectra were recorded from 200 nm to320 nm with a scan speed of 200 nm/min with a
98   spectral bandwidth of 10 nm using a JASCON CD spectrophotometer (Maryland, USA). Three
99   scans were averaged to plot the spectra. Concentration of single/double stranded/calf thymus
100 DNA was kept constant at 50 μM and its spectrum was read between 220 and 300 nm.
101 Increasing concentrations of chrysomycin A (0-220μM) were added to DNA and the change in
102 CD spectra was recorded, and the graph was plotted using Graphpad prism version 7 software.
103 The spectra of buffer solution (5mMTris-HCl, pH 8.0) containing chrysomycin A at appropriate
104 concentrations were subtracted from the spectra of DNA and chrysomycin A-DNA complex.

Interaction of chrysomycin A with single/double stranded oligonucleotides

106 Antibiotics and drugs with antimicrobial activity that have preferences for DNA sequences were
107 identified from published literature [15, 16], and a random set of oligonucleotides was synthesized as
108 short stretches (single stranded) and were used in fluorescence spectrometry as described earlier
109 (section 5.1.1). The most preferred sequences were identified based on the highest fluorescence
110 read out. After identifying these sequences, short oligos of DNA sequences were synthesized and
111 ligated to prepare double stranded DNA, and were used in the fluorescence spectrometry and
112 circular dichroism studies.

Molecular docking analysis

114 Protein structures, 5D5H (*M. tuberculosis* topoisomerase I), 5BTD (*M. tuberculosis* gyrase); and

115 DNA structures, IBNA (dodecamer without ACGT site) and IHQ7 (with ACGT site) were

116 retrieved from PDB (protein data bank) database in PDB format. The ligands attached with the

117 protein were removed using PrepWizard software in Schrondinger suites 2019-1. Energy

118 minimization was carried out along with optimizations such as building missing loops and

119 removal of water molecules. SiteMap was used to predict the ligand binding sites and the

120 catalytic domain was selected. Two dimensional structure of chrysomycin A (CID 73468) was

121 retrieved from PubChem database and imported to LigPrep software of the suite and energy

122 minimizations were performed. Finally, with the default setting of 15Å X 15Å X 15Å grid

123 points, a grid was generated. This was used in the docking analysis using Glide dock-XP mode

124 (extra precision).

Mobility shift assay

126 To 200 ng of plasmid DNA (pBR322), chrysomycin A was added at different concentrations (0 –

127 10 µM) and allowed to interact. From each of these reactions, 10 µL of the mix was run on a 1%

128 agarose gel (prepared in 1X Tris acetate buffer, pH 8.0) for 60 min at 50 V/cm in 1X Tris acetate

129 buffer containing ethidium bromide. The DNA band pattern was documented using Bio-Rad gel

130 documentation system.

Scanning electron microscopy

132 Fifty microliter of *M. tuberculosis* H37Rv culture (of McFarland standard 1.0 treated with

133 chrysomycin A at 1X MIC overnight, and untreated control) was centrifuged at 8000 g for 10

134 min at 25 °C. The resulting pellet was washed with ice-cold 1X PBS and suspended in 1.0 mL of

135 Dubos Difco broth. Two hundred microliter of this suspension was loaded onto polylysine-

136 coated cover slips that were prepared according to manufacturer's protocol (Sigma-Aldrich). The

137 bacteria were allowed to settle on the cover slip for 30 min. Then, the culture was decanted

138 gently and 2.5% glutaraldehyde in PBS (pH 7.4) was added to the coverslip. This was incubated

139 overnight at 4 °C and then subjected to dehydration with a series of ethanol concentrations (50%,

140 70%, 90% and 100%). At each step of ethanol gradient treatment, 10 min of incubation was

141 provided for effective dehydration. The coverslips were dried at room temperature and the

142   samples were gold-sputtered using JEOL-1200 (Peabody, MA, USA) and imaged using a JEOL-

143   JSM-5600 LV (USA) scanning electron microscope.

M. tuberculosis topoisomerase I inhibition assay

145   *M. tuberculosis* topoisomerase I enzyme was procured from Inspiralis, UK. Supercoiled pUC19

146   plasmid was isolated using either a plasmid maxiprep kit (Magerey Nagel) or using a modified

147   method described by Carbone et al. 2012 using miniprep kit (Magerey Nagel). Two units of the

148   enzyme were used in each reaction to relax the supercoiled DNA in the presence of different

149   concentrations of chrysomycinA (10, 20, 40 and 80 μM). Experimental procedures were

150   followed as per the protocol provided by the manufacturer.

M. tuberculosis gyrase inhibition assay

152   *M. tuberculosis* gyrase enzyme was purchased from Inspiralis, UK. In decatenation assay

153   kinetoplast DNA served as the substrate (every reaction had 200 ng of DNA). Chrysomycin A at

154   different concentrations (5, 50 and 100 μM) was used to inhibit the enzyme function.

155   Supercoiling assay had relaxed topoisomers of pBR322 plasmid (provided in the kit) as

156   substrate, and the assay was carried out in the presence of ATP (1 mM). Chrysomycin A (5, 50

157   and 100 μM) was used to inhibit the enzyme function. For DNA relaxation assay, pUC19

158   supercoiled plasmid (300 ng) was used as the substrate and the assay was performed without

159   ATP in the reaction. Ciprofloxacin at 25 μM and novobiocin at 20 μM served as positive control

160   for inhibition. Chrysomycin A at different concentrations (0-80 μM) was used to inhibit the

161   enzyme functions. In all reactions, except in the negative controls, 2 units of the enzyme was

162   used in the decatenation, supercoiling and relaxation assays. All procedures were followed as per

163   the protocol provided by the manufacturer.

Results and Discussion

Activity of chrysomycin A against drug resistant clinical strains of *M. tuberculosis*

166   The antimicrobial activity of chrysomycin A was tested on *M. tuberculosis* strains that were

167   resistant to different drugs and we tested if there is any change in their minimum inhibitory

168   concentrations (MIC). Interestingly, more than 70% of the drug resistant strains recruited were

169   inhibited at the same concentration of chrysomycin A at which it inhibited the susceptible

170 virulent laboratory strain *M. tuberculosis* H37Rv. The remaining strains were inhibited at slightly

171 higher concentrations. The details of the strains, their susceptibility to anti-TB drugs and the

172 MIC observed in the case of chrysomycinA are provided in Table 1.Strains 2-5 were resistant to

173 isoniazid, rifampicin and levoflaxocin while susceptible to kanamycin. However, chrysomycin A

174 elicited bactericidal activity on these strains below its MIC which was observed on *M.*

175 *tuberculosis* H37Rv. Strain 1 was similar to Strains 2-5 except that it was resistant to kanamycin

176 also. It was killed by chrysomycin A at the same MIC that killed *M. tuberculosis* H37Rv.On the

177 whole, chrysomycin A seemed to be very effective against MDR strains while it was less

178 effective on ofloxacin resistant strains suggesting that the molecule could act on topoisomerases.

Chrysomycin A exhibits synergistic activity with anti-tuberculosis drugs

180 To validate the observation on drug resistant strains of *M. tuberculosis*, chrysomycin A was

181 tested along with first-line and second-line anti-TB drugs and checked for their efficacy on

182 bacterial killing. *M. smegmatis* mc^{2}155, the surrogate mycobacterium, was treated with

183 chrysomycin A in combination with the first-line drugs rifampicin, isoniazid, ethambutol and

184 second-line drug ciprofloxacin and novobiocin. Figure S2 summarizes the result; briefly,

185 chrysomycin A acts synergistically with ethambutol, ciprofloxacin and novobiocin while it also

186 shows additive property in exerting antimicrobial activity in combination with rifampicin and

187 isoniazid. Chrysomycin A belongs to coumarin class of antibiotics which are known to bind

188 gyrase subunit B and inhibit the enzyme function. Interestingly, while acting in synergy the

189 amount of chrysomycin A and the combination drugs could be reduced by 4 fold to effect the

190 same level of killing. Thus, it seems chrysomycin A could be inhibiting the topoisomerases along

191 with ciprofloxacin and novobiocin. Chrysomycin A showed synergism when treated along with

192 ethambutol, and it could be because the molecule might have secondary targets in the bacterium.

193 Isoniazid and ethambutol are known to act synergistically and are required only at half their

194 original MIC to cause bacterial killing [17]. However, in combination with chrysomycin A, only

195 one fourth the concentration is required to elicit the same bactericidal activity. Pyrazinamide was

196 not included in the study because it does not inhibit the growth of *M. smegmatis* [18].

Chrysomycin A – DNA interaction

Chrysomycin A intercalates DNA at specific sequences

7

199   The planar structure of chrysomycin A (Figure S3) and the speculation on its ability to bind

200   DNA warranted DNA interaction studies. The intrinsic fluorescence of chrysomycin A facilitated

201   the drug-DNA interaction studies through the analysis of alterations in the intrinsic fluorescence

202   after forming drug-DNA complex. Chrysomycin A emits fluorescence at 505 nm in TE buffer,

203   (pH 8.0) when excited at 280 nm or 400 nm. Making use of this property, the change in its

204   fluorescence was monitored with addition of increasing concentrations of calf thymus DNA to a

205   constant amount of chrysomycin A. We observed a concentration-dependent increase in

206   fluorescence of chrysomycin A on addition of calf thymus DNA (Figure1A). Also, a red shift (5

207   nm) was observed in the fluorescence emission after addition of DNA which indicated a complex

208   formation. The shift also shows that chrysomycin A is buried deep inside the hydrophobic DNA

209   helix which prevents its interaction with water molecules. This phenomenon was described by

210   Sirajuddin et al with other intercalating drugs [19]. The ratio of observed to initial fluorescence was

211   plotted against the respective concentration of DNA and a Stern-Volmer constant (Ksv) of 1.2 X

212    $10^4 \, M^{-1}$ was obtained from the slope of the graph (Figure 1B). The constant obtained matches

213   neither with the lower values of groove binders nor in the higher constants of canonical

214   intercalators (Ksv<10^4 if it is a groove binder, Ksv>10^5 in the case of intercalators) demanding a

215   quenching experiment to draw insights into the binding. Therefore to validate the mode of

216   binding, potassium iodide was introduced to quench the fluorescence of unbound and DNA-

217   bound chrysomycin A. Contrary to our expectation, on addition of potassium iodide we observed

218   an increase in fluorescence even from unbound chrysomycin A and the DNA-chrysomycin A

219   complex. A graph was plotted using the F/F_0 ratios versus the concentration of potassium iodide

220   added (Figure1C). A slope was calculated for both the linear graphs and it was found that the

221   difference in the Ksv (Stern-Volmer constant) was larger indicating that the interaction could be

222   through intercalation. To rule out the possibility of it being a groove binder, increasing

223   concentrations of sodium chloride was added to the DNA and DNA-chrysomycin A complex to

224   increase the ionic strength of the solution which would result in the removal of surface bound

225   molecules and consequently reduce fluorescence intensity. As expected, the fluorescence

226   intensity remained largely unaffected even after the addition of high concentrations of sodium

227   chloride (Figure1D). Further, circular dichroism spectrometry was performed to find

228   chrysomycin A-induced alterations in the secondary structure of DNA. A negative band around

229   245 nm and positive band around 275 nm are characteristic of B form of DNA (calf thymus

230   DNA). Alteration in the negative band would indicate a change in helicity, and alterations in the

231   positive band would indicate perturbation of the stacks in the DNA [20]. On treatment with

232   chrysomycin A, the negative band at 245 nm was altered which pointed out at a change in

233   helicity which in turn supported intercalation (Figure 1E). The positive band was disturbed only

234   when very high concentrations of chrysomycin A were added. In addition, to understand whether

235   the molecule could affect supercoiled form of DNA, pUC19 plasmid was treated with

236   chrysomycin A and electrophoresed on an agarose gel. As expected, the supercoiled form of

237   DNA band migrated slowly with increasing concentrations of chrysomycin A (Figure S1). This

238   shift in mobility was also observed by TT Wei et al[9] who studied interaction of intercalators with

239   plasmid DNA. Furthermore, through molecular docking, chrysomycin A was found to intercalate

240   through minor groove (Figure 1F).

241   Therefore, the above evidences confirm that chrysomycin A intercalates DNA with low Stern –

242   Volmer constant (Ksv). This also leads to a hypothesis that the lower affinity observed might be

243   due to chrysomycin A's preference for specific DNA sequences. By data mining the literature,

244   we could identify such small molecules that bind specific DNA sequences, and they are listed in

245   Supplementary Table 1.Some of those specific sequences were randomly chosen, synthesized

246   and we performed fluorescence spectrometry with chrysomycin A (5 μM).A concentration-

247   dependent increase in fluorescence was observed upon addition of increasing amounts of

248   oligonucleotides, and a significant variation in fluorescence was observed based on the sequence

249   of the oligonucleotides (Figure 2A). This varied fluorescence symbolizes preference for specific

250   sequences. On comparing the sequences, it was found that a GC flanked by A and T appeared to

251   be the most preferred sequence for binding of chrysomycin A. To validate this observation,

252   double stranded DNA oligos with increasing number of AGCT and ACGT sites were

253   synthesized and fluorescence spectroscopy analysis was carried out. As expected, there was an

254   increase in fluorescence depending on the increasing number of AGCT/ACGT sites (Figure 2B

255   and 2D). Change in the secondary structure was also monitored for each of these oligos through

256   circular dichroism spectrometry (Figure 2C and 2E). A significant change was observed in the

257   helicity (increasing negative band at 245 nm) only when there was a single AGCT/ACGT site.

258   Also, oligos containing single ACGT was observed to be more vulnerable to chrysomycin A than

259   those containing AGCT in terms of alterations in the DNA structure. However, this change was

260   not observed in DNA with more than one AGCT/ACGT sites. This is presumed to be due to a

261   stabilization effect of saturated DNA–chrysomycin A complex which does not allow any more
262   change in the secondary structure. To confirm these results, molecular docking was performed
263   with DNA sequences with and without the ACGT sites (1HQ7 and IBNA, respectively) (Figure
264   3). Docking scores were ten-fold high (-5) in the case of binding to DNA with ACGT site
265   compared to DNA without ACGT site. Also, chrysomycin A intercalated through the major
266   groove in ACGT-containing DNA compared to the minor groove intercalation with DNA lacking
267   ACGT. Hoechst 33238 and ethidium bromide served as controls which have no sequence
268   specificity for binding. Next, in pursuit of finding the significance of the ACGT/AGCT sites, we
269   found an orphan ACGT site in the strong topoisomerase sites (STS) of topoisomerase I of *M.*
270   *smegmatis* and *M. tuberculosis* [21]. Interestingly, we found that actinomycin D also exhibits
271   sequence specific binding and binds preferentially to GC flanked by A and T regions of DNA [16,
272   22] and, actinomycin D also restricts topoisomerase I activity in tumor cells [23]. Therefore we
273   wished to test if chrysomycin A also could possibly inhibit topoisomerases of *M. tuberculosis*.
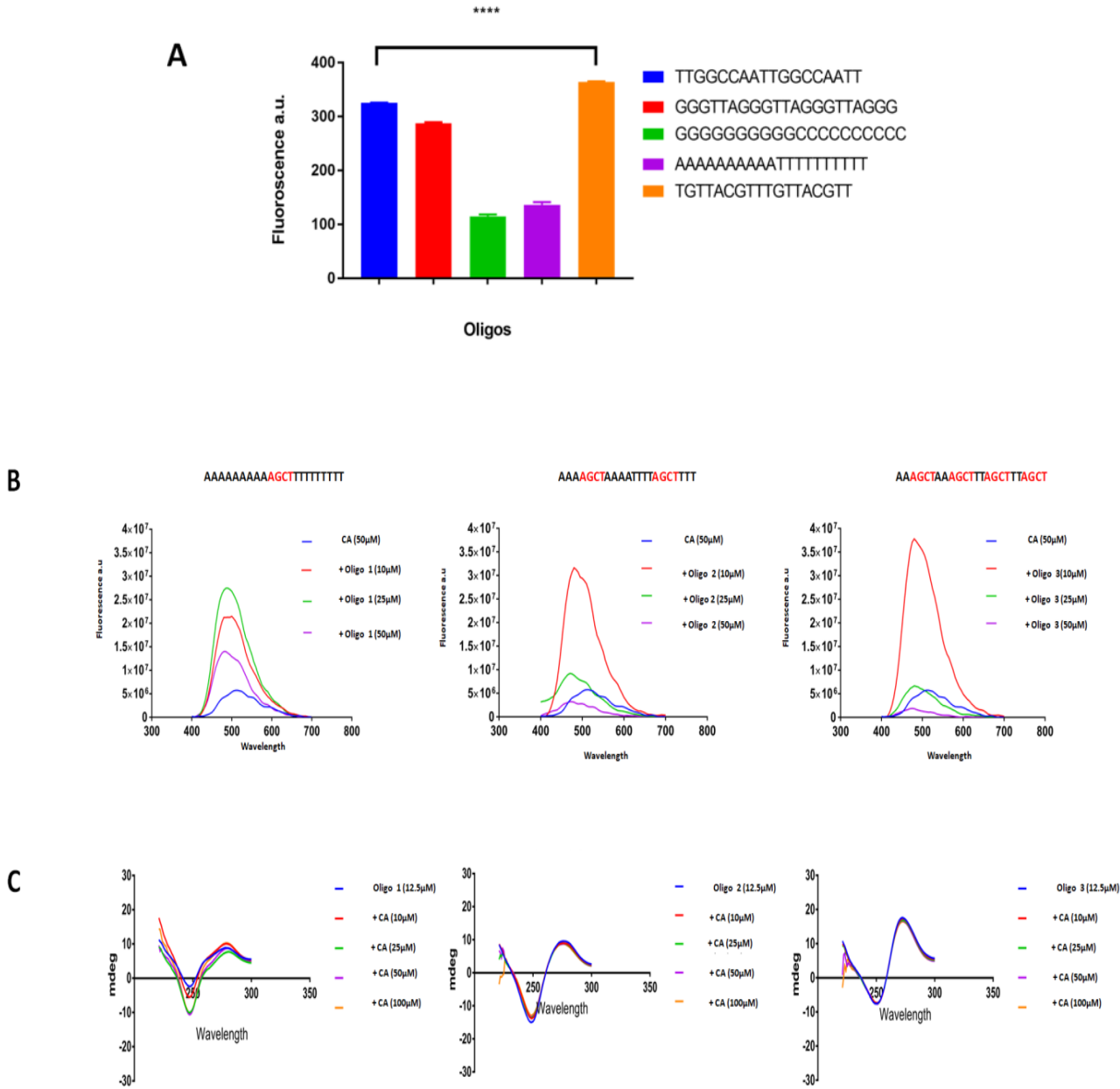
Chrysomycin A inhibits the activity of topoisomerases of *M. tuberculosis*

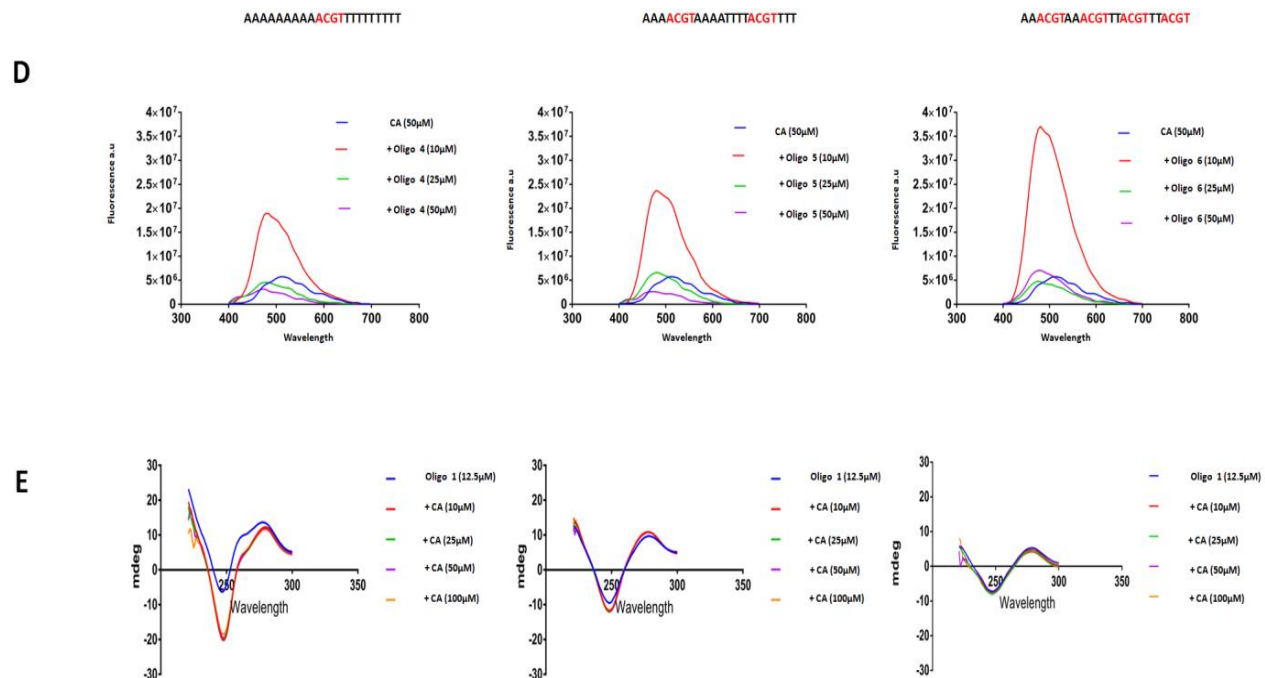275   Ahmed et al. [24] observed that conditional knocking down of topoisomerase I in *M. tuberculosis*
276   resulted in the bacterial shrinkage as well as de-compaction of the genetic materials. A
277   comparable observation was made by Arjomandzadegan et al [25], where a drug resistant strain of
278   *M. tuberculosis* treated with ofloxacin (fluoroquinolone that inhibits gyrase enzyme activity)
279   acquired a shrunken abnormal oval shape. Thus, it is evident that inhibition of topoisomerases
280   results in the reduction of bacterial size. To find the effect of chrysomycin A on *M. tuberculosis*
281   morphology, the bacterium was treated with chrysomycin A at its MIC for 12 h and subjected to
282   scanning electron microscopy. We observed 5 to 10 fold reduction in the size of chrysomycin A-
283   treated bacteria when compared to the untreated control (Figure 4A and 4B). We also observed
284   that small rod-shaped bacteria failed to grow further when we tried to retrieve them in an
285   antibiotic-free growth medium. Altogether, the change in morphology hinted at a possible
286   topoisomerase inhibition. In addition, chrysomycin A belongs to coumarin class of antibiotics
287   and coumarins are known for their anti-gyrase activity by binding to the ATP binding subunit B,
288   and therefore we wondered if chrysomycin A might inhibit the gyrase enzyme. Also, we have
289   already shown that it can intercalate at specific sequences in DNA, and intercalators are well
290   known inhibitors of topoisomerase enzymes.

10

291   We used Schrondinger docking software to check whether chrysomycin A can bind to *M.*
292   *tuberculosis* topoisomerase I (PDB ID: 5D5H) and *M. tuberculosis* gyrase (PDB ID: 5BTD).
293   Interestingly, chrysomycin A was found to interact with the primase domain of the
294   topoisomerase I enzyme and the active site Tyr-342 [26] was found to interact with the molecule
295   (Figure 4C and 4D). We did not observe any such interaction in the docking study with the
296   gyrase enzyme. Subsequently, a DNA relaxation assay was performed with *M. tuberculosis*
297   topoisomerase I with (0-80 μM) and without chrysomycin A. As expected a concentration-
298   dependent inhibition of relaxation was observed (Figure 4E). At 20 μM, chrysomycin A seemed
299   to inhibit almost half of the enzyme activity. Furthermore, to the best of our knowledge this IC_{50}
300   value of 20 μM seems to be the best among any natural molecule with the same activity. The
301   molecule was also tested for inhibition of various functions of *M. tuberculosis* gyrase. The
302   molecule could inhibit decatenation activity (5 μM) efficiently but exhibited moderate to poor
303   inhibition of the DNA supercoiling (50 μM) and DNA relaxation activity (50 μM) of the gyrase
304   enzyme (Figure 5A, 5B and 5C). We speculate that the gyrase inhibition is through its DNA
305   intercalation rather than through direct binding to the enzyme. Thus, these observations
306   supported our hypothesis that chrysomycin A can inhibit both the topoisomerase I and gyrase
307   enzymes of *M. tuberculosis*.

308

11
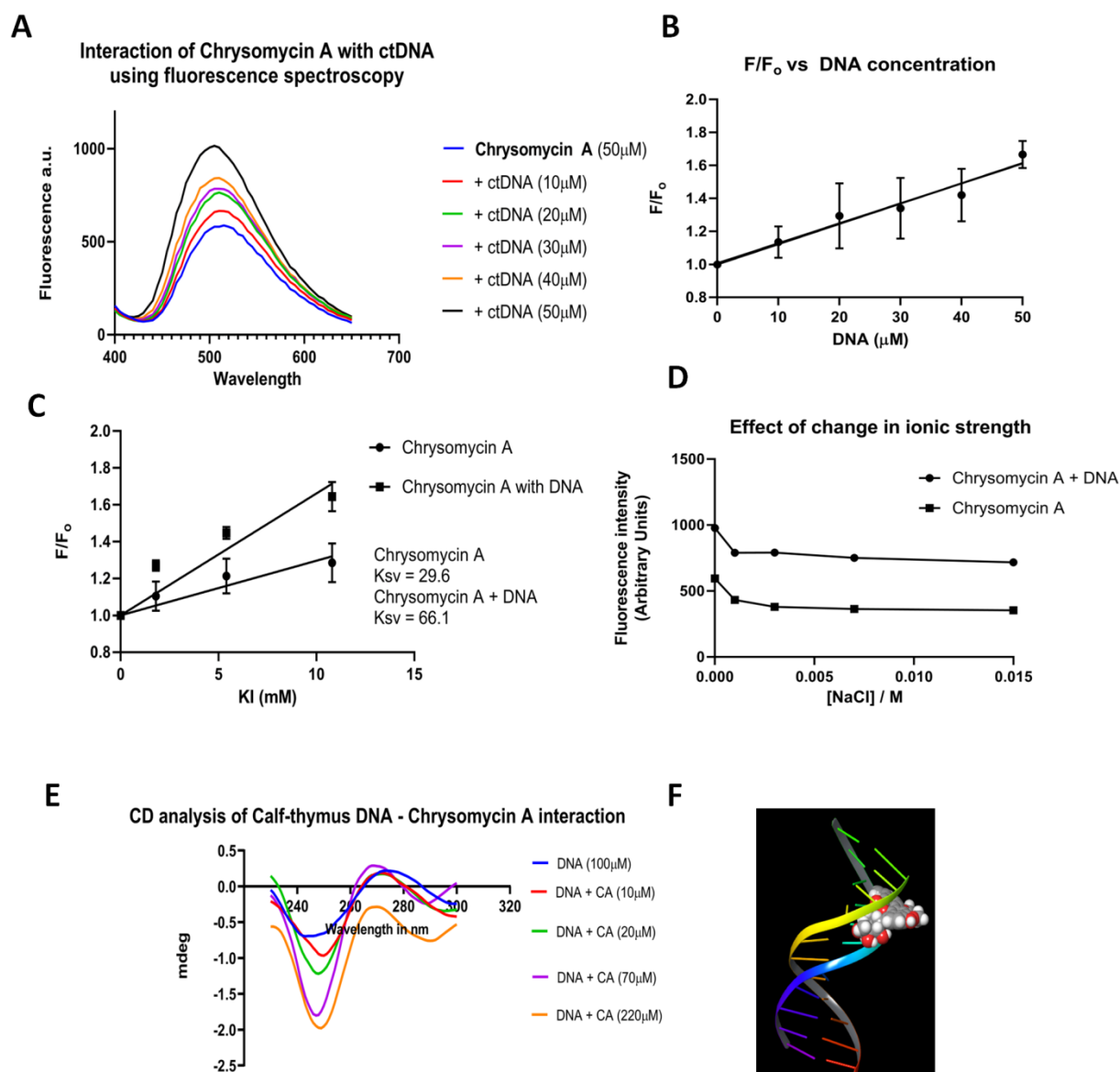
Figure 1: **A**. Change in fluorescence of chrysomycinA on addition of calf thymus DNA. **B.** Determination of Stern-Volmer constant (K_{SV}) for DNA-chrysomycin A complex. **C.** Comparison of K_{SV} of free chrysomycin A and DNA-bound chrysomycin A, using potassium iodide as the quencher. **D.** Effect of change in ionic strength on fluorescence of DNA-chrysomycinA complex. **E.** Circular dichroism spectrometry of DNA-chrysomycinA complex. **F.** Molecular docking analysis: chrysomycin A docked onto IBNA.

A

Oligos

- TTGGCCAATTGGCCAATT
- GGGTTAGGGTTAGGGTTAGGG
- GGGGGGGGGGGCCCCCCCCCC
- AAAAAAAAAATTTTTTTTTT
- TGTTACGTTTGTTACGTT

317

318

B

AAAAAAAAAAAGCTTTTTTTTTT   AAAAGCTAAAATTTAGCTTTT   AAAGCTAAAGCTTTAGCTTTAGCT


C

319

13

320

321

Figure 2: Chrysomycin A preferentially binds to specific nucleotide sequences. A. Fluorescence spectrometry shows differential fluorescence emission of chrysomycinA bound to different nucleotide sequences. B. Change in fluorescence with respect to the number of AGCT sites in the oligos. C. Circular dichroism spectrometry shows changes in the secondary structure of DNA bound to chrysomycin A with respect to the number of AGCT sites in the oligos. D. Change in fluorescence with respect to the number of ACGT sites in the oligos. E. Circular dichroism spectrometry shows changes in the secondary structure of DNA bound to chrysomycin A with respect to the number of ACGT sites in the oligos.

330

331

332
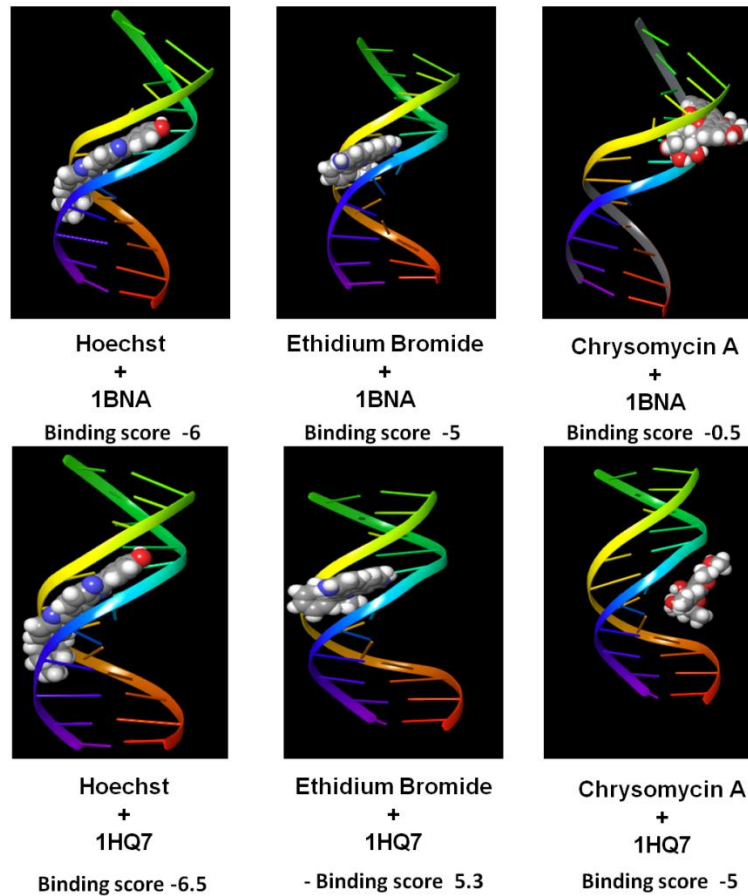
Figure 3: Molecular docking of chrysomycin A, ethidium bromide and Hoechst with DNA
sequences with ACGT (1HQ7) and without ACGT (1BNA) site.

335

336
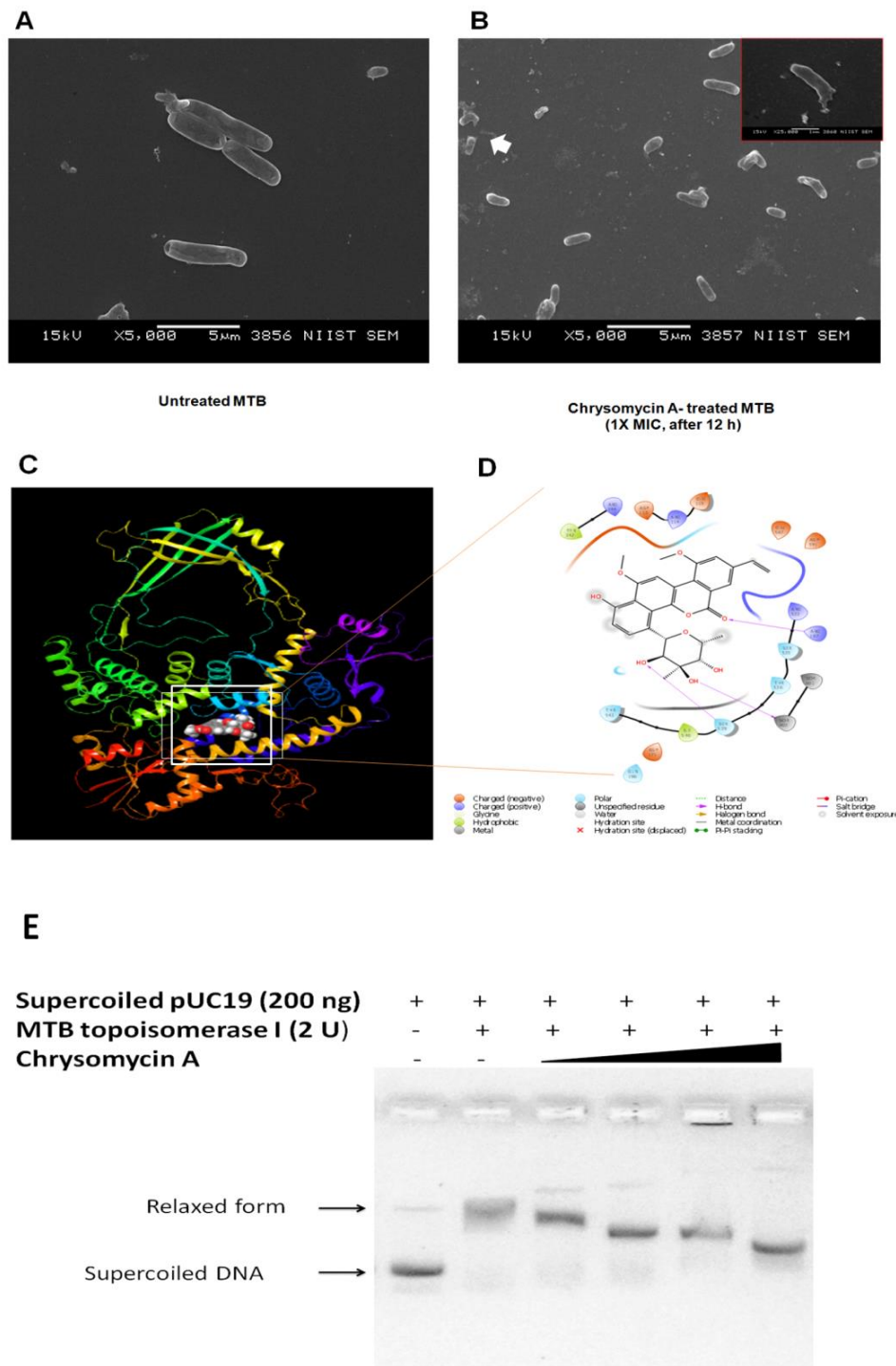
Figure 4: Chrysomycin A interacts with *M. tuberculosis* topoisomerase I to inhibit the growth of the bacteria. A and B are SEM images of untreated and chrysomycin A-treated bacteria, respectively. The inset image in B shows a broken leaky bacterium. C. Molecular docking of chrysomycin A bound to *M. tuberculosis* topoisomerase I protein. D. The binding pocket of

342 chrysomycin A in the protein shows the interacting amino acids. E. DNA relaxation assay with

343 *M. tuberculosis* topoisomerase I and chrysomycin A.
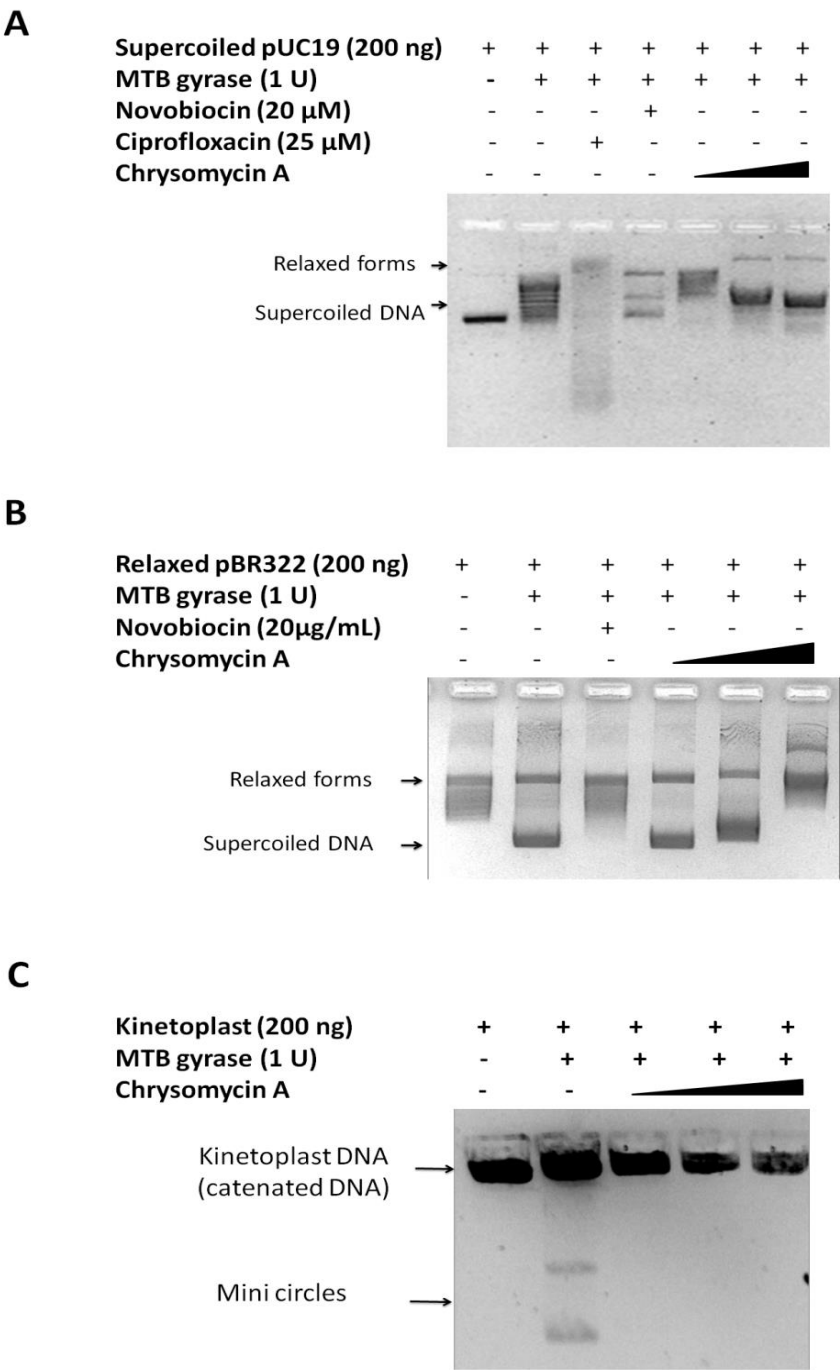
344

345 **Figure 5**: Gyrase inhibition assay. A - DNA relaxation assay. B - DNA supercoiling assay. C -

346 Decatenation assay.

Table 1: Antimicrobial activity of chrysomycin A against drug resistant clinical strains of *M. tuberculosis.*

Strain*	Resistant to	Susceptible to	MIC(µg/ml)
1	INH, RMP, Km, LFX	No data	4
2	INH, RMP, LFX	Km	2
3	INH, RMP, LFX	Km	4
4	INH, RMP, LFX	Km	1
5	INH, RMP, LFX	Km	1
6	INH, RMP, Km	LFX	2
7	INH, RMP, EMB, M, Ofx	Km, Ak, M	8
8	INH, Ofx	RMP, Km	16
9	INH, RMP, EMB, M, Ofx	Km,Ak, M	8
10	INH	RMP, Km,Ofx	16
11	RMP	INH, EMB,Km,Ak, M, Ofx	1
12	INH, RMP,Ofx	EMB,Km,Ak, M	16
13	RMP, Km	INH, EMB, Ofx, Ak, M	8
14	STR, INH, RMP, EMB, Ofx	Km	1
15	INH, RMP, EMB, Ofx	Km, Ak, M, Ofx	16
16	STR,INH, RMP	EMB,Km,Ofx	16
17	STR,INH, RMP, EMB,	Km, Ofx	2
18	INH	RMP, EMB,Km,Ofx,Ak, M	4

18

19	INH, RMP,Km,LFX	STR,EMB,Ak	4
20	INH, RMP, Km,	STR, LFX	2
H37Rv	-		4

349 INH – Isoniazid, RMP – Rifampicin, EMB – Ethambutol, Ofx – Ofloxacin, LFX – Levofloxacin,

350 STR – Streptomycin, Km – Kanamycin, M –Moxifloxacin, Ak – Amikacin.

351 * - identity of the clinical isolates withheld.

Conclusion

353 Chrysomycin A inhibits most of the drug resistant clinical strains of *M. tuberculosis* and acts in
354 synergy with ethambutol, the first line drug and ciprofloxacin, the second line drug.
355 Chrysomycin A inhibits the activity of topoisomerase I and gyrase enzymes of *M. tuberculosis* to
356 kill the bacterium. The inhibition activity was either by binding to the primase domain of the
357 topoisomerase I, or by binding to specific nucleotide sequences of DNA which are apparently the
358 recognition and binding sites of the topoisomerase I, thereby preventing the enzyme activity.

Acknowledgement:

367 **Conflict of interests**: The authors declare no conflict of interests.

References

369 1.   Strelitz F, Flon H, Asheshov INJJob. Chrysomycin: a new antibiotic substance for
370 bacterial viruses. 1955; **69**: 280.

2.   Jain SK, Pathania AS, Parshad R et al. Chrysomycins A–C, antileukemic naphthocoumarins from Streptomyces sporoverrucosus. *RSC advances* 2013; **3**: 21046-53.

3.   MATSON JA, ROSE WC, BUSH JA et al. Antitumor activity of chrysomycins M and V. *The Journal of antibiotics* 1989; **42**: 1446-8.

4.   Weiss U, Yoshihira K, Highet R et al. The Chemistry of the Antibiotics Chrysomycin A and B Antitumor Activity of Chrysomycin A. *The Journal of antibiotics* 1982; **35**: 1194-201.

5.   Wada S-i, Sawa R, Iwanami F et al. Structures and biological activities of novel 4'-acetylated analogs of chrysomycins A and B. 2017; **70**: 1078-82.

6.   Muralikrishnan B, Dan VM, Vinodh J et al. Anti-microbial activity of chrysomycin A produced by Streptomyces sp. against Mycobacterium tuberculosis. 2017; **7**: 36335-9.

7.   Wu F, Zhang J, Song F et al. Chrysomycin A derivatives for the treatment of multi-drug-resistant tuberculosis. 2020; **6**: 928-38.

8.   Greenstein M, Monji T, Yeung R et al. Light-dependent activity of the antitumor antibiotics ravidomycin and desacetylravidomycin. *Antimicrobial agents and chemotherapy* 1986; **29**: 861-6.

9.   Wei TT, BYRNE KM, WARNICK-PICKLE D et al. Studies on the mechanism of action of gilvocarcin V and chrysomycin A. *The Journal of antibiotics* 1982; **35**: 545-8.

10.   Caleffi-Ferracioli KR, Maltempe FG, Siqueira VLD et al. Fast detection of drug interaction in Mycobacterium tuberculosis by a checkerboard resazurin method. *Tuberculosis* 2013; **93**: 660-3.

11.   Palomino J-C, Martin A, Camacho M et al. Resazurin microtiter assay plate: simple and inexpensive method for detection of drug resistance in Mycobacterium tuberculosis. *Antimicrobial agents and chemotherapy* 2002; **46**: 2720-2.

12.   Rehman SU, Sarwar T, Husain MA et al. Studying non-covalent drug–DNA interactions. *Archives of biochemistry and biophysics* 2015; **576**: 49-60.

13.   Husain MA, Ishqi HM, Sarwar T et al. Interaction of indomethacin with calf thymus DNA: a multi-spectroscopic, thermodynamic and molecular modelling approach. *MedChemComm* 2017; **8**: 1283-96.

14.   Sadeghi M, Bayat M, Cheraghi S et al. Binding studies of the anti-retroviral drug, efavirenz to calf thymus DNA using spectroscopic and voltammetric techniques. *Luminescence* 2016; **31**: 108-17.

15.   Chang Y-M, Chen CK-M, Hou M-H. Conformational changes in DNA upon ligand binding monitored by circular dichroism. *International journal of molecular sciences* 2012; **13**: 3394-413.

16.   Hampshire AJ, Fox KR. The effects of local DNA sequence on the interaction of ligands with their preferred binding sites. *Biochimie* 2008; **90**: 988-98.

17.   Zhu C, Liu Y, Hu L et al. Molecular mechanism of the synergistic activity of ethambutol and isoniazid against Mycobacterium tuberculosis. *Journal of Biological Chemistry* 2018; **293**: 16741-50.

18.   Zhang Y, Scorpio A, Nikaido H et al. Role of acid pH and deficient efflux of pyrazinoic acid in unique susceptibility of Mycobacterium tuberculosis to pyrazinamide. *Journal of bacteriology* 1999; **181**: 2044-9.

19.   Sirajuddin M, Ali S, Badshah A. Drug–DNA interactions and their study by UV–Visible, fluorescence spectroscopies and cyclic voltametry. *Journal of Photochemistry and Photobiology B: Biology* 2013; **124**: 1-19.

416 20.   Kypr J, Kejnovská I, Renčiuk D et al. Circular dichroism and conformational
417 polymorphism of DNA. *Nucleic acids research* 2009; **37**: 1713-25.
418 21.   Sikder D, Nagaraja V. Determination of the recognition sequence of Mycobacterium
419 smegmatis topoisomerase I on mycobacterial genomic sequences. *Nucleic acids research* 2000;
420 **28**: 1830-7.
421 22.   Van Dyke MW, Hertzberg RP, Dervan PB. Map of distamycin, netropsin, and
422 actinomycin binding sites on heterogeneous DNA: DNA cleavage-inhibition patterns with
423 methidiumpropyl-EDTA. Fe (II). *Proceedings of the National Academy of Sciences* 1982; **79**:
424 5470-4.
425 23.   Trask D, Muller M. Stabilization of type I topoisomerase-DNA covalent complexes by
426 actinomycin D. *Proceedings of the National Academy of Sciences* 1988; **85**: 1417-21.
427 24.   Ahmed W, Menon S, Godbole AA et al. Conditional silencing of topoisomerase I gene of
428 Mycobacterium tuberculosis validates its essentiality for cell survival. *FEMS microbiology*
429 *letters* 2014; **353**: 116-23.
430 25.   Arjomandzadegan M, Sadrnia M, Titov L et al. Transmission Electron Microscopy of
431 XDR Mycobacterium tuberculosis Isolates Grown on High Dose of Ofloxacin. *Scientia*
432 *pharmaceutica* 2017; **85**: 3.
433 26.   Godbole AA, Ahmed W, Bhat RS et al. Targeting Mycobacterium tuberculosis
434 topoisomerase I by small-molecule inhibitors. *Antimicrobial agents and chemotherapy* 2015; **59**:
435 1549-57.

436

437